IL NUOVO CIMENTO **47 C** (2024) 79
DOI 10.1393/ncc/i2024-24079-x

Colloquia: IFAE 2023

Measurement of the High Mass Drell-Yan process in di-tau final states and leptoquark searches with the ATLAS experiment at the LHC(*)

G. Padovano([1])([2]) on behalf of the ATLAS Collaboration

([1]) *Dipartimento di Fisica, Sapienza Università di Roma - Roma, Italy*
([2]) *INFN, Sezione di Roma - Roma, Italy*

received 13 February 2024

Summary. — Leptoquarks constitute one of the most prominent candidates in the context of new physics models interpreting B physics anomalies recently measured in the Standard Model flavour sector. An analysis is presented, searching for leptoquark particles through the precision study of the Drell-Yan process with tau leptons in the final state, performed by the ATLAS Collaboration, exploiting 139 fb^{-1} of pp collision data from the LHC. The full analysis strategy is outlined and projections of the final exclusion limit on leptoquark models are reported.

1. – The flavour anomalies as a hint for new physics

Interest has been raised recently in the flavour sector of the Standard Model (SM), as some anomalous measurements (the so-called *flavour anomalies*), constitute a promising handle to build new physics models, alternative to the traditional way to access new physics through addressing the Higgs hierarchy problem. The flavour anomalies represent a set of measurements, mainly exploiting semi-leptonic B mesons decays, and showing tension or disagreement with the SM predictions. Such measurements usually consist in branching-fractions, or ratios of branching-fractions, evaluated across different leptonic decay channels to test lepton universality. The current overall picture of flavour anomalies includes past measurements from the BaBar and Belle experiments together with recent results from the LHCb experiment [1-5], and globally hints for the presence of new physics lightly and universally coupled to leptons and quarks of first and second family and more strongly coupled to leptons of the third family, thus violating SM lepton universality in the third generation [6, 7].

One of the most prominent explanations of flavour anomalies is given by leptoquark models, predicting new exotic particles (the *leptoquarks*) involved in interaction vertices coupling both leptons and quarks [8]. In pp collisions, leptoquarks can be either singly or pair produced, or can be exchanged in the non-resonant t-channel. They can be either scalar (spin 0) or vector (spin 1), although the vector leptoquark model is the most promising candidate to explain the flavour anomalies [9, 10].

This report presents a search for leptoquark particles, exploiting the Drell-Yan process with tau leptons in the final state, performed by the ATLAS Collaboration [11], using the 139 fb^{-1} dataset of pp collisions from the LHC [12] at a centre-of-mass energy of

(*) IFAE 2023 - "Energy Frontier" session

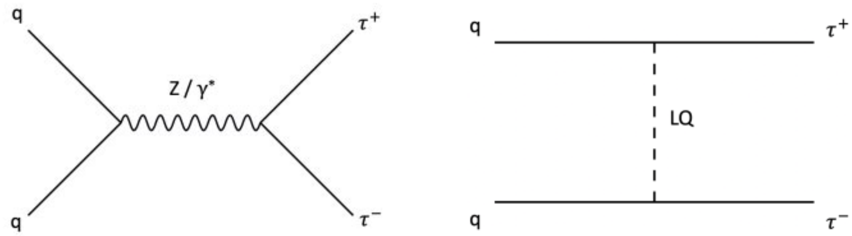

(a) Di-tau Drell-Yan process. (b) Di-tau LQ mediated diagram.

Fig. 1. – Feynman diagrams for the processes involved in the analysis: (a) the SM Drell-Yan process and (b) the exotic LQ mediated process.

$\sqrt{s} = 13$ TeV. In the following, the analysis strategy is outlined, including background estimation and systematic uncertainty evaluation. Projections of the expected sensitivity for leptoquark model exclusion are finally given.

2. – The High Mass Drell-Yan analysis

The analysis is focused on the Drell-Yan process with tau leptons in the final state, represented in fig. 1(a), which is used as a probe to search for leptoquark particles (LQ). Leptoquarks, in fact, are involved in a t-channel exchange diagram (fig. 1(b)), yielding the same di-tau final state, accompanied by two b-jets coming from the proton or from gluon splitting in the initial state. Being the final state exactly the same, interference effects may occur between the exotic leptoquark t-channel and the SM Drell-Yan diagrams, producing a deviation in the Drell-Yan cross-section measurement with respect to the SM value, which should be particularly evident in the high-mass tail of the differential distribution $d\sigma/dm_{\tau\tau}$, for hypothetical leptoquark particles with mass of $O(1$ TeV$)$.

2˙1. *Analysis strategy and Monte-Carlo background modelling.* – Tau leptons can decay leptonically into electrons or muons $\tau \to \ell\nu_\ell$ ($\ell = e, \mu$) or hadronically $\tau \to \pi^-\nu_\tau$, $\tau \to \pi^-\pi^+\pi^-\nu_\tau$. Leptonic tau decays are reconstructed as ordinary electrons or muons, accompanied by missing energy, while hadronic decays are reconstructed as narrow jets. This analysis exploits both the semi-leptonic channel, in which one tau decays leptonically and the other hadronically, and the fully hadronic channel, where both taus decay hadronically.

The signal region is defined by basic selections on the quality of involved objects, electrons, muons, hadronic tau jets, and requiring a high combined invariant mass of the di-tau system, $m_{\tau\tau} > 100$ GeV. After these basic selections, the major backgrounds of the analysis can be seen in fig. 2, showing sensible kinematic variables, and consists of $t\bar{t}$ production, Z+jets production, multiboson and the background from quark- or gluon-initiated jets misidentified as hadronic taus, referred to as fake τ_{had} background. Control regions are defined requiring final states with two electrons and two muons and are used to validate the corresponding $Z \to ee$ and $Z \to \mu\mu$ backgrounds in the signal region. A *same-sign* validation region, in which the two taus are required to have the same charge, is defined to check the data-driven fake τ_{had} background estimate, as will be further detailed in sect. **2**˙2.

All regions are further split into event categories according to number of b-tagged jets (0, 1, ≥ 2 b-jets), to exploit different background composition evolving with b-jets multiplicity.

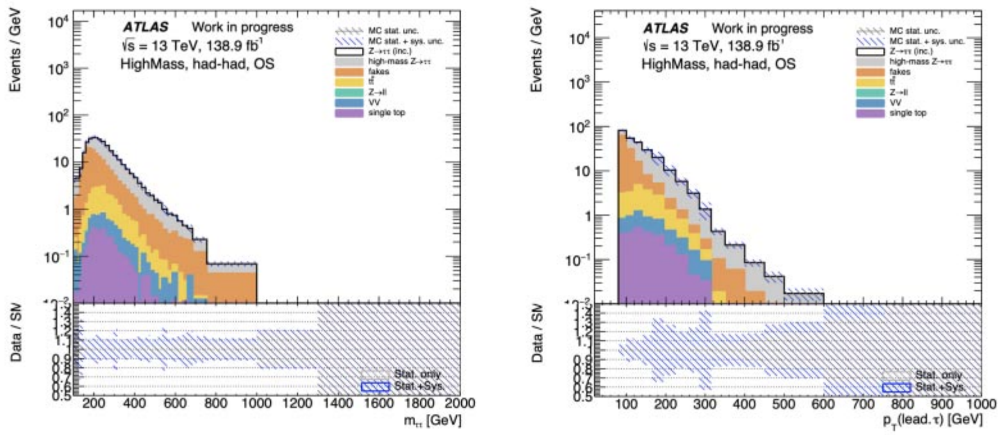

(a) (b)

Fig. 2. – Data over Monte-Carlo comparisons in the OS signal region for two sensible kinematic variables: the di-tau invariant mass (a) and the leading tau p_T (b). Data are not shown as the signal region is currently blinded.

2˙2. *Data-driven fake* τ_{had} *background estimate*. – One of the most significant background processes in this analysis, playing a major role in the fully hadronic channel, comes from the so-called *fake hadronic taus*, and consists of events in which at least one hard quark or gluon jet is misidentified as a hadronic tau. This background is estimated via a data-driven technique, as Monte-Carlo simulation is not able to properly represent multi-jet events.

A tau anti-ID control region is defined in correspondence to the analysis signal region, as having exactly the same requirements except for a reversed requirement on the tau identification criterion (*i.e.*, enriched in jets faking taus). Fake-factors are defined as transfer factors from the anti-ID SR to the ID SR:

$$FF = \frac{N_{ID}}{N_{antiID}} \; .$$

Fake-factors are measured in proper control regions, defined to be enriched in quark or gluon jets, and a combined fake-factor is derived as a linear combination of the primitive fake-factors with coefficients representing the fractions of quark/gluon jets in the signal region of the analysis. More precisely, the combined fake-factors have been evaluated implementing the following model

$$FF_{comb} = \alpha_q FF_q + \alpha_g^{ljvt} FF_g^{ljvt} + (1 - \alpha_q - \alpha_g^{ljvt}) FF_g^{hjvt} \; , \tag{1}$$

where the FF_q, FF_g^{ljvt}, FF_g^{hjvt} are measured in regions enriched in quark or gluon jets (with low/high jet vertex tagging score [13]) respectively, and the α fractions are measured via a template fit done on the tau width kinematic variable. Results of fake-factor calculation are shown in fig. 3. In particular, an example of template fit is shown in fig. 3(a), while combined fake-factors are shown in fig. 3(b), in bins of tau lepton p_T.

Once fake-factors are calculated, background extrapolation is done from data in the SR anti-ID to the SR ID. It can be shown that considering a di-tau final state in the fully

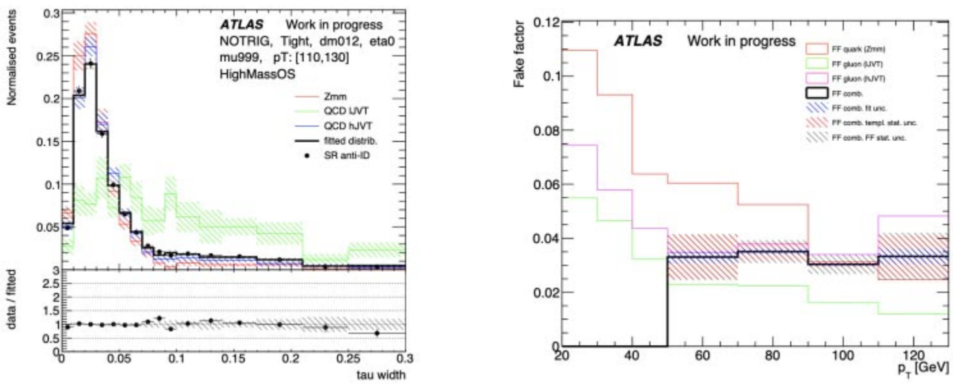

(a) (b)

Fig. 3. – Primitive and fitted tau-width templates (a), together with primitive and combined fake-factors (b). Template fits and fake-factors are evaluated in bins of p_T and several other sensible quantities.

hadronic channel, the number of background events in the SR is obtained according to the following expression:

$$N_{bkg} = \left[N(\tau_{antiID}\tau_{ID}) - N(\tau^t_{antiID}\tau^t_{ID})\right] FF_1 + \\ \left[N(\tau_{ID}\tau_{antiID}) - N(\tau^t_{ID}\tau^t_{antiID})\right] FF_2 - \\ \left[N(\tau_{antiID}\tau_{antiID}) - N(\tau^t_{antiID}\tau^t_{antiID})\right] FF_1 FF_2 \ , \tag{2}$$

where $N(\tau_{antiID}\tau_{ID})$ is the number of events with leading tau anti-identified and subleading tau identified (estimated from data), $N(\tau^t_{antiID}\tau^t_{ID})$ is the same number of events with the additional requirement of taus being truth-matched (estimated via Monte-Carlo) and similar definitions hold for all the other sub/superscripts combinations. In this notation $FF_{1,2}$ represent the fake-factors evaluated in the p_T bin of the anti-identified tau.

A simpler expression holds in the semileptonic channel, which coincides with the first term only of eq. (2), as in that channel only the first lepton can be a fake hadronic tau, if leptons are ordered by decreasing flavour. Results of the extrapolations are shown in fig. 4, where closure between data and a stack of Monte-Carlo and background of fake hadronic taus is observed in the same-sign region, where both leptons have the same charge, built to be enriched in fake hadronic taus.

The systematic uncertainties on the background of fake taus have also been evaluated, and recognised as coming mainly from the statistical uncertainties of the primitive fake-factors and of the primitive templates, together with the uncertainties coming from the templates fitting procedure (*i.e.*, the uncertainties on the α parameters, together with their correlation).

2˙3. *Systematic uncertainties.* – The main systematic uncertainties have been identified and considered in the measurement. Experimental systematic uncertainties concern the major objects characterising the signal and the backgrounds entering the signal region. In particular, uncertainties on taus (energy scale, energy resolution), muons (identification, sagitta), electrons (energy scale, resolution), jets (energy scale, eta intercalibration, flavour composition) have been considered, showing a global impact of $\approx 10\%$.

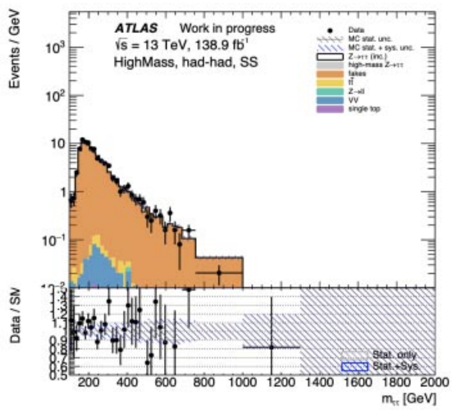

Fig. 4. – Fakes background extrapolation in the same-sign validation region. Closure between data and Monte-Carlo and fakes is observed in the di-tau invariant mass variable.

Modelling uncertainties, representing theory imprecision attributed to the Monte-Carlo simulation, have also been considered. Uncertainty bands have been extracted comparing several Monte-Carlo generators, differing in matrix-element calculation or in parton shower modelling, concerning mainly the $Z \to \tau\tau$, $Z \to \ell\ell$ ($\ell = e, \mu$), $t\bar{t}$, single-top processes.

2˙4. *Expected exclusion limit evaluation.* – Exclusion limits on several leptoquark models can be obtained through a profile likelihood fit approach. The exclusion limit evaluation is done considering jointly both the semi-leptonic and fully hadronic channels, to use all the available statistical power, exploiting signal region separation in categories of b-jets and the di-tau invariant mass a sensible variable. Both scalar and vector leptoquark models are investigated for several leptoquark mass hypotheses.

Projections of the final exclusion achievable on vector leptoquark models by an LHC experiment with 139 fb^{-1} of data has been evaluated in ref. [10] as an exclusion contour in the LQ mass (M_U) *versus* coupling constant (g_U) plane, as shown in fig. 5. As this analysis is sensible to the non-resonant t-channel leptoquark exchange, we expect exclusions at higher LQ masses for high values of the coupling constant, with respect to the exclusion obtainable by analyses probing LQ pair-production. The exclusion contour is expected to be very near the region of phase space representing leptoquark models suitable to explain the flavour anomalies, which is $g_U \approx 1 - 1.5$ and $M_U \approx 1 - 2$ TeV.

3. – Conclusions and future perspectives

An analysis searching for leptoquark particles thought the di-tau Drell-Yan process has been presented, in the context of new physics models addressing the B meson anomalies measured in the flavour sector of the Standard Model, performed with the ATLAS experiment at the LHC. The measurement strategy has been outlined, covering all major aspects for the analysis, and projections of the final exclusion contour for vector leptoquark models has been reported.

As a future development of this work, alongside with the actual leptoquark exclusion limits, the ATLAS Collaboration is foreseeing to publish an unfolded precision measurement of the di-tau differential Drell-Yan cross section. This measurement, once obtained,

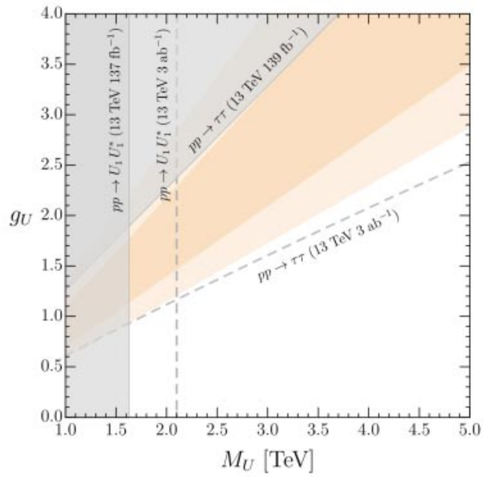

Fig. 5. – Expected exclusion contours for vector LQ models with 13 fb^{-1} of data and 3 ab^{-1} of data. Exclusions for LQ pair-production are also shown [10].

will be compared with the unfolded cross section already performed in the di-electron and di-muon channels, providing further test of lepton universality across the three families.

REFERENCES

[1] Seuthe A., *Lepton flavour universality tests at LHCb*, in *Proceedings of 57th Rencontres de Moriond on QCD and High Energy Interactions, La Thuile, Italy, 25 Mar–1 Apr 2023.*
[2] LHCb Collaboration, *Phys. Rev. Lett.*, **131** (2023) 051803, arXiv:2212.09152.
[3] LHCb Collaboration, *Phys. Rev. Lett.*, **128** (2022) 191803.
[4] LHCb Collaboration, *JHEP*, **06** (2014) 133, arXiv:1403.8044.
[5] LHCb Collaboration, *Phys. Rev. Lett.*, **126** (2021) 161802, arXiv:2012.13241.
[6] Aebischer J., Isidori G., Pesut M., Stefanek B. A. and Wilsch F., *Eur. Phys. J. C*, **83** (2023) 153, arXiv:2210.13422.
[7] Greljo A., Salko J., Smolkovič A. and Stangl P., *JHEP*, **05** (2023) 087, arXiv:2212.10497.
[8] Schmaltz M. and Zhong Y. M., *JHEP*, **01** (2019) 132, arXiv:1810.10017.
[9] Angelescu A., Bečirević D., Faroughy D. A., Jaffredo F. and Sumensari O., *Phys. Rev. D*, **104** (2021) 055017, arXiv:2103.12504.
[10] Cornella C., Faroughy D. A., Fuentes-Martin J., Isidori G. and Neubert M., *JHEP*, **08** (2021) 050, arXiv:2103.16558.
[11] ATLAS Collaboration, *JINST*, **3** (2008) S08003.
[12] Evans L. and Bryant P., *JINST*, **3** (2008) S08001.
[13] ATLAS Collaboration, *Forward jet vertex tagging using the particle flow algorithm*, ATL-PHYS-PUB-2019-026, `https://cds.cern.ch/record/2683100`.